

Cite this: *Anal. Methods*, 2023, 15, 6435

# Accurate selected ion flow tube mass spectrometry quantification of ethylene oxide contamination in the presence of acetaldehyde

Stefan J. Swift,<sup>a</sup> Kseniya Dryahina,<sup>a</sup> Ann-Sophie Lehnert,<sup>b</sup> Nicholas Demarais,<sup>c</sup> Vaughan S. Langford,<sup>c</sup> Mark J. Perkins,<sup>d</sup> Leslie P. Silva,<sup>e</sup> Maroua Omezzine Gnioua<sup>af</sup> and Patrik Španěl<sup>ga</sup>

In September 2020, traces of ethylene oxide (a toxic substance used as a pesticide in developing countries but banned for use on food items within the European Union) were found in foodstuffs containing ingredients derived from imported sesame seed products. Vast numbers of foodstuffs were recalled across Europe due to this contamination, leading to expensive market losses and extensive trace exposure of ethylene oxide to consumers. Therefore, a rapid analysis method is needed to ensure food safety by high-throughput screening for ethylene oxide contamination. Selected ion flow tube mass spectrometry (SIFT-MS) is a suitable method for rapid quantification of trace amounts of vapours in the headspace of food samples. It turns out, however, that the presence of acetaldehyde complicates SIFT-MS analyses of its isomer ethylene oxide. It was proposed that a combination of the  $\text{H}_3\text{O}^+$  and  $\text{NO}^+$  reagent ions can be used to analyse ethylene oxide in the presence of acetaldehyde. This method is, however, not robust because of the product ion overlaps and potential interferences from other matrix species. Thus, we studied the kinetics of the reactions of the  $\text{H}_3\text{O}^+$ ,  $\text{NO}^+$ ,  $\text{OH}^-$  and  $\text{O}^-$  ions with these two compounds and obtained their rate coefficients and product ion branching ratios. Interpretation of these experimental data revealed that the  $\text{OH}^-$  anions are the most suitable SIFT-MS reagents because the product ions of their reactions with acetaldehyde ( $\text{CH}_2\text{CHO}^-$  at  $m/z$  43) and ethylene oxide ( $\text{C}_2\text{H}_3\text{O}_2^-$  at  $m/z$  59) do not overlap.

Received 20th June 2023  
Accepted 9th November 2023

DOI: 10.1039/d3ay01036h

rsc.li/methods

## 1. Introduction

A strained ring structure cyclic ether and the simplest epoxide, ethylene oxide ( $\text{C}_2\text{H}_4\text{O}$ ), is used in the chemical industry to manufacture ethylene glycols.<sup>1,2</sup> Recently, quantitation of ethylene oxide in polysorbates has been demonstrated using selected ion flow tube-mass spectrometry (SIFT-MS).<sup>3,4</sup> Ethylene oxide is also used for sterilisation purposes, having been used in the medical industry to sterilise surgical equipment<sup>5,6</sup> and often used as a fumigant<sup>7–9</sup> on plants and foods against insects and other organisms. This is due to its effectiveness as a toxic agent against pests<sup>10</sup> and its relatively low cost.<sup>11</sup> Its use as a fumigant is however banned across the EU<sup>2,12</sup> due to its

toxicity,<sup>13</sup> as well as its carcinogenic<sup>13,14</sup> and mutagenic<sup>14,15</sup> characteristics. Ethylene oxide is also classed by the United States Environmental Protection Agency (US EPA) as a class 1 mutagen.<sup>16</sup> In high amounts, ethylene oxide exposure<sup>17</sup> is known to cause acute symptoms including vomiting, nausea, headaches, as well as other chronic symptoms.<sup>18</sup> In much lower doses, ethylene oxide has been reported to still be harmful to health due to its high reactivity,<sup>13</sup> genotoxicity,<sup>19</sup> and alkylating ability with DNA's nucleophilic sites<sup>20</sup> through an  $\text{S}_\text{N}^2$  reaction pathway<sup>21,22</sup> (without the need for ethylene oxide to be metabolically activated).<sup>23,24</sup> The European maximum residue level of ethylene oxide in seeds, nuts and herbs is currently  $0.05 \text{ mg kg}^{-1}$ ,<sup>2</sup> and in fruit and vegetables is even lower at  $0.02 \text{ mg kg}^{-1}$ .<sup>25</sup>

Despite the stringent regulations within the EU controlling the use of ethylene oxide (and other contaminants) on food produced within this economic area, much produce available to purchase in the western world often originates from countries with less stringent regulations. An important example of when ethylene oxide contamination may take place within foodstuffs is in the case of sesame seeds. Recently it was reported that  $30 \text{ mg kg}^{-2}$  of ethylene oxide was present in sesame seeds imported into Belgium from India.<sup>2</sup> This caused wide-spread

<sup>a</sup>J. Heyrovský Institute of Physical Chemistry of the CAS, v. v. i., Dolejškova 2155/3, Prague 182 23, Czechia. E-mail: patrik.spanel@jh-inst.cas.cz<sup>b</sup>Syft Technologies, Hilperstraße 31, Darmstadt 64295, Germany<sup>c</sup>Syft Technologies, 68 Saint Asaph Street, Christchurch Central City, Christchurch 8011, New Zealand<sup>d</sup>Element Lab Solutions, Unit 4, Wellbrook Court, Girton Rd, Girton, Cambridge CB3 0NA, UK<sup>e</sup>Syft Technologies, 675N Euclid St #627, Anaheim, CA 92801, USA<sup>f</sup>Faculty of Mathematics and Physics, Charles University, Ke Karlovu 3, Prague 121 16, Czechia

alarm across Europe and caused the mass recall of food products that may have been contaminated with ethylene oxide,<sup>2,12,26</sup> leading to massive economic consequences for the businesses involved. Thus, there is an urgent need to monitor ethylene oxide residue in foods.

The main technique used to date to analyse ethylene oxide is based on dispersive solid phase extraction (dSPE) combined with gas chromatography – tandem mass spectrometry (GC-MS/MS). This process is labour intensive even though the retention time for ethylene oxide is less than 3 minutes.<sup>27</sup> The use of the SIFT-MS approach would reduce both the sample processing time and analysis time. Thus, we set out to investigate whether ethylene oxide could be quantified in food products by selected ion flow tube mass spectrometry (SIFT-MS), a soft chemical ionisation technique based on the kinetics of ion–molecule reactions between selected reagent ions and analyte molecules present in sampled air with well-defined reaction times.<sup>28</sup> This task is complicated by the fact that ethylene oxide is isomeric with acetaldehyde (commonly found in food products and in the atmosphere)<sup>29,30</sup> and thus product ion overlaps are likely and should be avoided for practical robust analyses.

Traditionally, the SIFT-MS has only been able to exploit three positive reagent ions ( $\text{H}_3\text{O}^+$ ,  $\text{NO}^+$  and  $\text{O}_2^+$ ) for analyses, but in recent years five new negative ions ( $\text{OH}^-$ ,  $\text{O}_2^-$ ,  $\text{O}^-$ ,  $\text{NO}_2^-$  and  $\text{NO}_3^-$ ) have become available, further enhancing its selectivity. Thus, we have studied the reactions of ethylene oxide and acetaldehyde with positive ( $\text{H}_3\text{O}^+$ ,  $\text{NO}^+$ ,  $\text{O}_2^+$ ) and negative ( $\text{O}^-$ ,  $\text{OH}^-$ ,  $\text{O}_2^-$ ,  $\text{NO}_2^-$  and  $\text{NO}_3^-$ ) reagent ions to determine their rate coefficients and product ion branching ratios. Using these kinetics data, it will be possible to quantify ethylene oxide in the presence of acetaldehyde. Note that whilst the ion–molecule reactions of a range of reagent ions ( $\text{Ar}^+$ ,  $\text{N}_2^+$ ,  $\text{NH}^+$ ,  $\text{NH}_2^+$ ,  $\text{NH}_3^+$  and  $\text{HCNH}^+$ ) with ethylene oxide have been investigated previously using the selected ion flow tube (SIFT) technique,<sup>31</sup> the data for the SIFT-MS reagent ions have not yet been reported in the scientific literature.

The quantification of ethylene oxide in the presence of acetaldehyde may be possible in some matrices by combining the use of  $\text{H}_3\text{O}^+$  and  $\text{NO}^+$  reagent ions in analyses,<sup>3</sup> although this method will be prone to interferences. Thus, in the present study, we explore the use of the negative reagent ions. Much of the earlier literature on ion–molecule reaction kinetics reports results obtained using a *Profile 3* instrument, whilst the recent literature increasingly covers the Voice200 series.<sup>32</sup> The rate constants and branching ratios of the product ions are already known for the reactions of the positive reagent ions  $\text{H}_3\text{O}^+$ ,  $\text{NO}^+$  and  $\text{O}_2^+$  with acetaldehyde.<sup>33</sup> However, for ethylene oxide, these values were used in the Syft Voice200 series kinetics library and so far to the best of our knowledge have not yet been reported in any academic publication. The main objective of the present study was to carry out the detailed characterisation of the reactions of the SIFT-MS negative reagent ions ( $\text{OH}^-$ ,  $\text{O}_2^-$ ,  $\text{O}^-$ ,  $\text{NO}_2^-$  and  $\text{NO}_3^-$ ) with ethylene oxide and acetaldehyde, with the objective of proposing a robust and accurate quantification method of ethylene oxide in the presence of acetaldehyde based on the available SIFT-MS reagent anions.

## 2. Materials and methods

### 2.1 Voice200infinity and materials

In this work we have used the latest model in the Voice200 series of instruments, the Voice200infinity (Syft Technologies Limited, Christchurch, New Zealand), to conduct this ion–molecule reaction kinetics study. Reagent ions generated in the ion source are injected into the flow tube individually in a fast sequence, switching between the reagent ions within three groups:  $\text{H}_3\text{O}^+$ ,  $\text{NO}^+$  and  $\text{O}_2^+$  are generated in the positive ion source conditions;  $\text{OH}^-$  and  $\text{O}_2^-$  are generated in the negative mode from moist air; and  $\text{O}^-$ ,  $\text{NO}_2^-$  and  $\text{NO}_3^-$  are generated in the negative mode from dry air.<sup>34</sup> A nitrogen carrier gas (purity 4.6, Messer Technogas, Prague, Czechia) has been used in these studies due to the demise of He as the carrier of choice for the SIFT-MS technique (because of its cost and renewability). The instrument keeps the sample gaseous by heating the inlet cone and capillary to 323 K, which directs the sample flow rate of 26 sccm into a flow tube (at 393 K and 460 mTorr).

The analytes used for the ion–molecule reaction kinetics study were acetaldehyde ( $\geq 99.5\%$ , Sigma-Aldrich, Steinheim, Germany) and ethylene oxide (from a permeation tube provided by Syft Technologies). Gaseous mixtures for this study were prepared in Nalophan bags filled with dry clean air (from a zero-air generator, UHP-10ZA-S, Parker, Gateshead, United Kingdom) by injecting several millilitres of the analyte headspace using plastic gas-tight syringes (Omnifix®, B. Braun, Bad Arolsen, Germany). During the measurements the samples were at room temperature.

As the air from the zero-air generator contains an impurity of  $\text{CO}_2$ , which also has a molecular weight of  $44 \text{ g mol}^{-1}$ , we investigated its effect by using cylinder nitrogen (purity 4.6) to fill Nalophan bags during sample preparation.

### 2.2 Branching ratios

Full scan (FS) mass spectra of air samples containing acetaldehyde and ethylene oxide at several concentrations were first separately collected in the  $m/z$  range 15 to 250 for all available reagent ions and compared with the corresponding blank spectra obtained using  $\sim 2 \text{ L}$  Nalophan bags containing zero-air only. Full scans were collected with a measurement time limit of 200 ms and an ion count limit of 10 000. This  $m/z$  range was chosen as it allowed for the identification of any secondary products, including dimers and adducts. The main product ions were identified from the FS spectra and a set of  $m/z$  values of interest were imported into a selected ion monitoring (SIM) method.

A set of seven arbitrary concentrations of acetaldehyde and ethylene oxide were analysed using the SIM method, which acquired 80 data points for each cycle for each reagent ion experiment, with measurement time limits of 100 ms and a count limit of 10 000 (allowing for much higher precision in measurements). The separate concentration levels were achieved by starting with a high concentration of acetaldehyde or ethylene oxide and diluting the sample for each consecutive measurement. The collected SIM data were exported to excel



files as raw signals per cycle. Average values for each of the selected ion signals for each concentration were calculated from 75 points (avoiding the first five measurement cycles to avoid any transition effects when switching the ion source mode from dry to wet).

Correlation analysis was conducted between the separate product ion counts and their total to identify which products were primary or secondary. In cases where there were several branches for the primary reaction, the branching ratios for the primary products were obtained as intercepts of the plots of the product ion count rate branching percentages, *versus* the total product ion signal at the limit of zero concentration by the commonly used extrapolation procedure.<sup>35,36</sup>

### 2.3 Reaction rate coefficients

The reaction rate coefficients were determined relatively to the rate coefficients for the proton transfer reactions of  $\text{H}_3\text{O}^+$  with acetaldehyde and ethylene oxide, which are assumed to be collisional,  $k_c$ .<sup>37</sup> This is because the exothermicities of these reactions are above  $40 \text{ kJ mol}^{-1}$ .<sup>36,38</sup> The rate coefficients for the other reagent ions were determined from the relative values of the ratios of the product ion and the reagent ion count rates calculated at the different concentrations of the analyte vapours. These ratios obtained for each reagent ion were plotted against those obtained for  $\text{H}_3\text{O}^+$  for different vapour concentrations. This allowed for a comparison of the slopes, directly proportional to the relative rate coefficients of the reactions. The reaction rate coefficients were then obtained by multiplying the relative rate values by the  $k_c$  for  $\text{H}_3\text{O}^+$ .<sup>37</sup> The  $k_c$  values for  $\text{H}_3\text{O}^+$  were calculated for 393 K using the polarizabilities and dipole moments of acetaldehyde and ethylene oxide given in Table 2.<sup>39</sup>

### 2.4 Limits of detection and quantification

The limits of detection (LOD) were determined from multiple blank measurements obtained by sampling from a clean glass bottle with zero-air passing through it. A series of measurements were conducted across the different reagent ions of interest for ethylene oxide and acetaldehyde (separately). The concentration values were reported by the *Voice200infinity* in ppb (according to the updated kinetics library using the values from this work). The standard deviation was taken of the concentrations reported by the *Voice200infinity* for each reagent ion. The standard deviation was then multiplied by 3.3 to obtain the LOD; multiplied by 10 to obtain the limit of quantification (LOQ).

### 2.5 Density functional theory (DFT) calculations of enthalpies

DFT calculations were conducted to evaluate whether the thermodynamics of the investigated reactions would likely result in formation of the hypothesised ionic structures, which would confirm the presence of a specific branching pathway occurring. All quantum chemistry calculations were performed using the ORCA 5.0.1 software.<sup>40</sup> Molecular geometries of all the neutral reactant molecules and of all the reagent and product ions were

first drawn using the AVOGADRO software<sup>41</sup> and were then further optimised using ORCA<sup>40</sup> with the B3LYP DFT method and the basis set 6-311++G(d,p), with D4 correction.<sup>42</sup> This level of theory was also used to calculate the normal mode vibrational frequencies and thermodynamic quantities of the neutral molecules, polarizability of ethylene oxide and the ion structures. The total enthalpies of all neutral molecules and ions (including several feasible structures of each of the product ions) were thus calculated for, as the sum of the total electronic energy ( $E_{\text{el}}$ ); the zero-point vibrational energy ( $E_{\text{ZPV}}$ ); the temperature-dependent portion of the vibrational energy ( $E_{\text{vib}}(T)$ ); and the thermal translational and rotational energies ( $5/2RT$ ) for standard temperature and pressure (298 K, 1 atm).

$$H = E_{\text{el}} + E_{\text{ZPV}} + E_{\text{vib}}(T) + 5/2 RT \quad (1)$$

The results are given as needed in the discussion of all the reactions.

## 3. Results and discussion

The following results were obtained under the conditions in which the *Syft Voice200infinity* instrument would be used routinely (*i.e.*, using an  $\text{N}_2$  carrier gas at 393 K).

### 3.1 Products and branching ratios

Full scan spectra were obtained using all reagents for ethylene oxide and acetaldehyde at several concentrations, to observe the product ions emerging from the background. The spectra for the  $\text{H}_3\text{O}^+$  and  $\text{OH}^-$  reagent ions are shown as examples in Fig. 1. It can be seen in this example that the reaction of  $\text{H}_3\text{O}^+$  with ethylene oxide produces  $m/z$  45 and its hydrate at  $m/z$  63 (as well as a small signal of the proton-bound dimer, at  $m/z$  89) whilst the  $\text{OH}^-$  reaction leads to a major increase in  $m/z$  59. Acetaldehyde, as expected, gives a very similar spectrum with  $\text{H}_3\text{O}^+$  but shows no signal of  $m/z$  59 with  $\text{OH}^-$ .

The inspection of these sets of spectra revealed that from all available reagent ions, only  $\text{H}_3\text{O}^+$ ,  $\text{NO}^+$ ,  $\text{OH}^-$  and  $\text{O}^-$  showed the potential for practical SIFT-MS analyses of ethylene oxide in the presence of acetaldehyde. This is because the  $\text{O}_2^{+}$  reaction leads to 30% of  $m/z$  43 and 70% of  $m/z$  44 products, which are known to overlap with the products of many other VOCs.  $\text{O}_2^-$ ,  $\text{NO}_2^-$  and  $\text{NO}_3^-$  do not react at any appreciable rate, thus the further detailed discussion within this publication only focuses on the  $\text{H}_3\text{O}^+$ ,  $\text{NO}^+$ ,  $\text{OH}^-$  and  $\text{O}^-$  reactions.

The branching ratios determined for these eight reactions are given in Table 1. Note that often the same product ions are observed for both acetaldehyde and ethylene oxide, albeit the branching ratios are in some cases different. The outstanding exception is the major product ion at  $m/z$  59 resulting from the  $\text{OH}^-$  reaction with ethylene oxide. The assignment of the  $m/z$  values reported in Table 1 will be discussed in Sections 3.3–3.6.

### 3.2 Reaction rate coefficients

The rate coefficients experimentally obtained in the present study for the reactions of interest are shown in Table 2 together



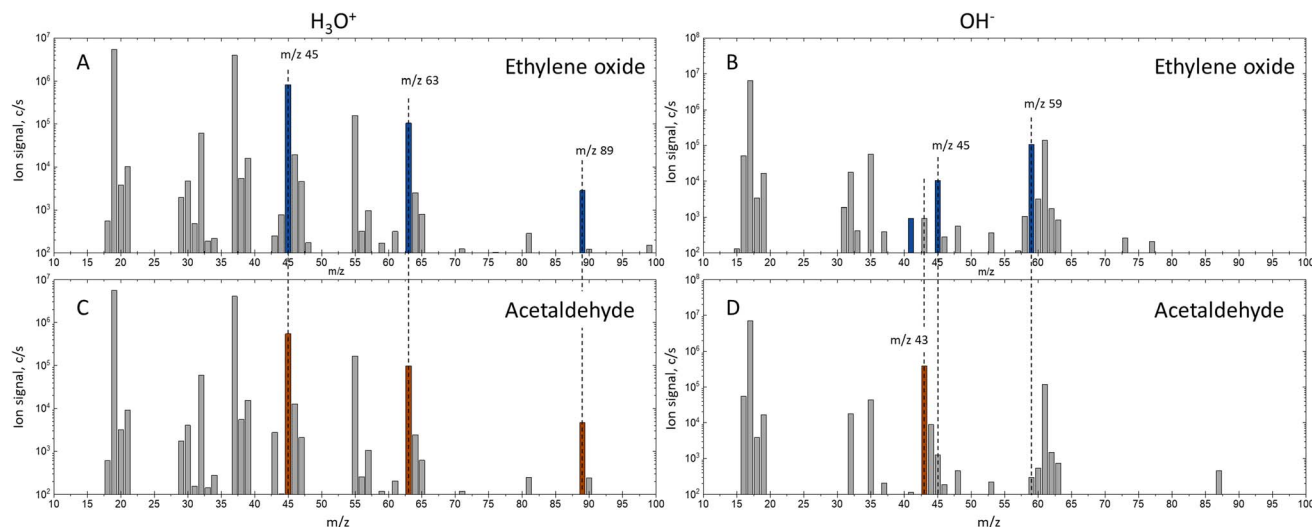


Fig. 1 Full scan spectra obtained for ethylene oxide using  $\text{H}_3\text{O}^+$  (A) and  $\text{OH}^-$  (B) and for acetaldehyde using  $\text{H}_3\text{O}^+$  (C) and  $\text{OH}^-$  (D).

Table 1 Branching ratios of the  $\text{H}_3\text{O}^+$ ,  $\text{NO}^+$ ,  $\text{OH}^-$  and  $\text{O}^-$  reactions with acetaldehyde and ethylene oxide. Values in bold show the major product ions

| Acetaldehyde (MW 44)   |   |                                       | Ethylene oxide (MW 44)                         |                           |  |
|------------------------|---|---------------------------------------|--|---------------------------|--|
| $\text{H}_3\text{O}^+$ | $\text{CH}_3\text{CHOH}^+$              | <i>m/z</i> 45 <b>100%</b>             | $\text{C}_2\text{H}_4\text{OH}^+$              | <i>m/z</i> 45 <b>100%</b> |  |
| $\text{NO}^+$          | $\text{CH}_3\text{CO}^+$                | <i>m/z</i> 43 <b>94%</b> <sup>a</sup> | $\text{C}_2\text{H}_3\text{O}^+$               | <i>m/z</i> 43 3%          |  |
|                        | $\text{CH}_3\text{CHO}\cdot\text{NO}^+$ | <i>m/z</i> 74 6%                      | $\text{C}_2\text{H}_4\text{O}\cdot\text{NO}^+$ | <i>m/z</i> 74 <b>97%</b>  |  |
| $\text{OH}^-$          | $\text{CH}_2\text{CHO}^-$               | <i>m/z</i> 43 <b>100%</b>             | $\text{C}_2\text{HO}^-$                        | <i>m/z</i> 41 5%          |  |
|                        |   |                                       | $\text{C}_2\text{H}_4\text{OH}^-$              | <i>m/z</i> 45 5%          |  |
|                        |   |                                       | $\text{C}_2\text{H}_3\text{O}_2^-$             | <i>m/z</i> 59 <b>90%</b>  |  |
| $\text{O}^-$           | $\text{C}_2\text{HO}^-$                 | <i>m/z</i> 41 8%                      | $\text{C}_2\text{HO}^-$                        | <i>m/z</i> 41 <b>96%</b>  |  |
|                        | $\text{C}_2\text{H}_3\text{O}^-$        | <i>m/z</i> 43 <b>65%</b>              | $\text{C}_2\text{H}_3\text{O}^-$               | <i>m/z</i> 43 4%          |  |
|                        | $\text{CO}_2\text{H}^-$                 | <i>m/z</i> 45 13%                     |  |                           |  |
|                        | $\text{C}_2\text{H}_3\text{O}_2^-$      | <i>m/z</i> 59 14%                     |  |                           |  |

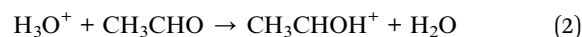
<sup>a</sup> In the present Syft library this is the only product.

with the previous literature values, where available. Note that  $\text{H}_3\text{O}^+$  reacts fast with both compounds, whilst the  $\text{NO}^+$  reaction is about five times lower than  $k_c$  for acetaldehyde and twenty times lower than  $k_c$  for ethylene oxide. Also, note that acetaldehyde reacts relatively fast with  $\text{OH}^-$  and only slowly with  $\text{O}^-$ . Ethylene oxide reacts with both  $\text{OH}^-$  and  $\text{O}^-$  at rate coefficients, which are around thirty times slower than  $k_c$ . Rate coefficients for the reactions of the other negative reagents with ethylene oxide and acetaldehyde were immeasurably slow.

### 3.3 $\text{H}_3\text{O}^+$ reactions

In the following sections, the reactions of the  $\text{H}_3\text{O}^+$  reagent ion with acetaldehyde and ethylene oxide are discussed separately. In both cases however, a single product was produced which was the protonated molecule at *m/z* 45.

**3.3.1 Acetaldehyde.** The single product resulting from the interaction of  $\text{H}_3\text{O}^+$  with acetaldehyde was the protonated molecule  $\text{CH}_3\text{CHOH}^+$  (*m/z* 45). This confirmed the previous results by Španěl *et al.* (1997).<sup>33</sup> The proton transfer reaction



is (according to our DFT calculations) exothermic by  $86 \text{ kJ mol}^{-1}$ , which is reasonably close to the proton affinity difference ( $768.5 - 691 = 77.5$ )  $\text{kJ mol}^{-1}$  (according to the NIST database).<sup>43</sup>

Note that a substantial signal of the single hydrate ion  $\text{CH}_3\text{CHOH}^+\text{H}_2\text{O}$  was also seen at *m/z* 63 and a much smaller signal of the secondary hydrate,  $\text{CH}_3\text{CHOH}^+(\text{H}_2\text{O})_2$  was seen at *m/z* 81. A proton-bound dimer ion  $\text{CH}_3\text{CHOH}^+\text{CH}_3\text{CHO}$  at *m/z* 89 was also present.

**3.3.2 Ethylene oxide.** Again, only one product for the  $\text{H}_3\text{O}^+$  reaction with ethylene oxide was observed, being  $\text{C}_2\text{H}_4\text{OH}^+$  at *m/z* 45, produced by proton transfer:



which is exothermic by  $84 \text{ kJ mol}^{-1}$  according to DFT; in good agreement with the proton affinity difference ( $774.2 - 691 = 83.2$ )  $\text{kJ mol}^{-1}$  (according to the NIST database).<sup>43</sup> Both the primary and secondary hydrates are observed, but in comparison with acetaldehyde the second hydrate signal is smaller. The signal of the proton bound dimer is similar to that of acetaldehyde. As a result, the  $\text{H}_3\text{O}^+$  mass spectra are almost identical for acetaldehyde and ethylene oxide (see Fig. 1).

### 3.4 $\text{NO}^+$ reactions

**3.4.1 Acetaldehyde.** The reaction of  $\text{NO}^+$  with  $\text{CH}_3\text{CHO}$  proceeds chiefly by hydride ion transfer with a small contribution of association:



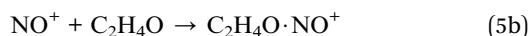
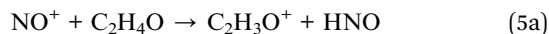
According to our DFT calculations both reaction channels are exothermic, (4a) by  $82 \text{ kJ mol}^{-1}$  and (4b) by  $176 \text{ kJ mol}^{-1}$ .



Note that the signal at  $m/z$  44 corresponds entirely to the  $^{13}\text{C}$  isotopologue of  $\text{CH}_3\text{CO}^+$ .

A minor adduct product ion (4b),  $\text{CH}_3\text{CHO}\cdot\text{NO}^+$  at  $m/z$  74 (branching ratio of 6%) was not reported previously in Španěl *et al.* (1997).<sup>33</sup> The reason for this difference is most likely down to the different carrier gases used in these studies –  $\text{N}_2$  used in this study is a more effective third body leading to observable association.

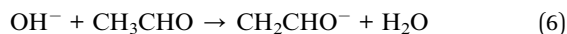
**3.4.2 Ethylene oxide.** Two products were detected in the  $\text{NO}^+$  reaction with  $\text{C}_2\text{H}_4\text{O}$ :



These were the hydride-transfer product at  $m/z$  43 ( $\text{C}_2\text{H}_3\text{O}^+$ , 3%); and the adduct ion at  $m/z$  74 ( $\text{C}_2\text{H}_4\text{O}\cdot\text{NO}^+$ , 97%), (Table 1). Note that charge transfer would be endothermic as the ionisation energy of  $\text{C}_2\text{H}_4\text{O}$  is 10.56 eV. In the DFT calculations the exothermicity of reaction (5a) was found to be 207  $\text{kJ mol}^{-1}$  for a particular structure  $[\text{H}_2\text{C}-(\text{C}=\text{O})-\text{H}]^+$ . The net reaction rate is only 4% of collisional and the main product is the adduct ion (5b). This therefore indicated that there are some barriers to hydride ion transfer, possibly related to the rearrangement needed.

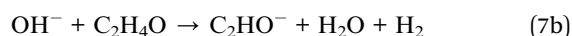
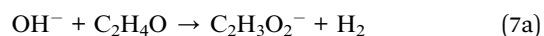
### 3.5 $\text{OH}^-$ reactions

**3.5.1 Acetaldehyde.** The  $\text{OH}^-$  reaction with acetaldehyde proceeds *via* proton transfer producing  $m/z$  43 only:



According to our DFT calculations this is exothermic by 106  $\text{kJ mol}^{-1}$  when the proton is taken from the methyl group. This reaction is relatively fast,  $k = 0.56 k_c$ . It is important to note that there is no product ion observed at  $m/z$  59, in stark contrast to ethylene oxide (see Fig. 1).

**3.5.2 Ethylene oxide.** As mentioned before, a surprising observation was that the major product ion of the  $\text{OH}^-$  reaction with ethylene oxide appeared at  $m/z$  59. This was confirmed independently on two Voice200-series instruments (Voice200*infinity* and Voice200*ultra* models) using separately sourced ethylene oxide standards. This  $\text{C}_2\text{H}_3\text{O}_2^-$  ion represents 90% of the branching pathway. In addition, there are product ions at  $m/z$  41 and  $m/z$  45 at 5% each. It should be noted that when much higher concentrations of ethylene oxide are introduced, the secondary product ion at  $m/z$  103 is detected, which corresponds to the addition of an ethylene oxide molecule to the ( $m/z$  59) product.



The product ion  $\text{C}_2\text{H}_3\text{O}_2^-$  has two different possible structures as shown in Fig. 2. These are the acetate anion (structure A) or an isomeric aldehyde anion (structure B).

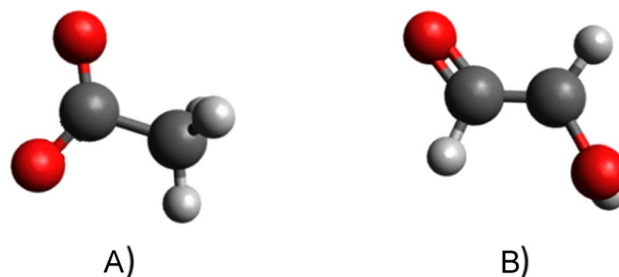


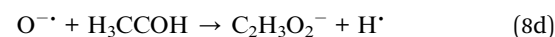
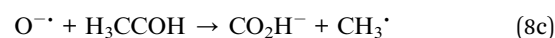
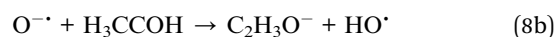
Fig. 2 Possible molecular structures of the  $\text{OH}^-$  ethylene oxide reaction product ions  $\text{C}_2\text{H}_3\text{O}_2^-$  (A) lower enthalpy, (B) higher enthalpy.

The exothermicity of reaction (7a) producing the structure shown in Fig. 2A is 337  $\text{kJ mol}^{-1}$  and is 136  $\text{kJ mol}^{-1}$  for the structure in Fig. 2B. This is due to the greater stabilisation of the singly bonded oxygen atom (Fig. 2A) to the carbon which also hosts a double bond to the second oxygen atom. The structure in Fig. 2B doesn't allow for this resonance stabilisation and therefore this less stable product is associated with a lower exothermicity of reaction, despite requiring less rearrangement from the reaction intermediate ion. Reaction (7a) however is certainly exothermic. The major product at  $m/z$  59 is thus a possible candidate for SIFT-MS ethylene oxide vapour concentration quantification because the rate coefficient of this reaction is  $k = 0.1 \times 10^{-9} \text{ cm}^3 \text{ s}^{-1}$ .

### 3.6 $\text{O}^{\cdot-}$ reactions

It can be seen in Table 1 that the major products of the  $\text{O}^{\cdot-}$  reactions with ethylene oxide and acetaldehyde are different ( $m/z$  41 and  $m/z$  43, respectively). This reagent ion thus could also potentially be used to separately quantify ethylene oxide and acetaldehyde. However, due to minor overlaps, the accurate quantification of ethylene oxide and acetaldehyde with  $\text{O}^{\cdot-}$  only is more complicated.

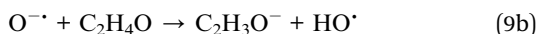
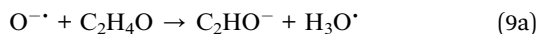
**3.6.1 Acetaldehyde.** The product ions listed by their  $m/z$  in Table 1 may be identified as various fragments and the reaction proceeds as:



Our DFT calculations showed that reaction channel (8a) with 8% branching ratio is slightly exothermic by 0.2  $\text{kJ mol}^{-1}$  to produce  $\text{H}_3\text{O}^{\cdot}$ , but would be endothermic by 44  $\text{kJ mol}^{-1}$  to produce separate  $\text{OH}^{\cdot}$  and  $\text{H}_2$  neutral molecules. The product of the main 65% channel (8b) results from proton transfer from acetaldehyde to  $\text{O}^{\cdot-}$  which is exothermic by 70  $\text{kJ mol}^{-1}$ . Note that the exothermicity of the 13% channel (8c) is 115  $\text{kJ mol}^{-1}$  and of the 14% channel (8d) is 225  $\text{kJ mol}^{-1}$ . The experimentally determined rate constant of the reaction of acetaldehyde with  $\text{O}^{\cdot-}$  is relatively slow (Table 2),  $k = 0.2 \times 10^{-9} \text{ cm}^3 \text{ s}^{-1}$ .

**3.6.2 Ethylene oxide.**  $\text{O}^{\cdot-}$  reacts with ethylene oxide as:





where the 96% channel (9a) corresponds to the formation of the ethynyloxy radical anion ( $\text{C}_2\text{HO}^-$ ), a process which is exothermic by  $125 \text{ kJ mol}^{-1}$  when producing  $\text{H}_3\text{O}^{\cdot}$  as the neutral product. The 4% channel (9b) is proton transfer which is exothermic by  $195 \text{ kJ mol}^{-1}$ . Despite the reaction exothermicity, a rate constant (even slower than for acetaldehyde) of  $k = 0.07 \times 10^{-9} \text{ cm}^3 \text{ s}^{-1}$  is observed which can be explained by the required atomic rearrangement and related presence of energy barriers.

### 3.7 Possible methods to individually analyse ethylene oxide and acetaldehyde in a mixture

**3.7.1 Quantification using  $\text{H}_3\text{O}^+$  and  $\text{NO}^+$ .** A method has previously been developed to quantify ethylene oxide in the presence of acetaldehyde using the  $\text{H}_3\text{O}^+$  and  $\text{NO}^+$  ions by Silva *et al.* (2022).<sup>3</sup> This quantification relies on proton transfer, eqn (2) and (3), and hydride ion transfer from acetaldehyde (4a). The method of quantifying ethylene oxide and acetaldehyde is based on the accurate measurement of  $m/z$  45 with  $\text{H}_3\text{O}^+$  and  $m/z$  43 with  $\text{NO}^+$ . The product ion signal at  $m/z$  45 is proportional to the sum of concentrations of ethylene oxide and acetaldehyde, each weighted by the corresponding rate coefficient (see Table 2). The acetaldehyde contribution can be estimated from the  $m/z$  43 signal obtained using the  $\text{NO}^+$  reagent ion. Linear combination of the  $\text{H}_3\text{O}^+$  and  $\text{NO}^+$  data can then be used to calculate the ethylene oxide concentration corrected for the presence of acetaldehyde.

This method may however be prone to inaccuracies due to common overlaps at  $m/z$  43, as many hydrocarbons frequently found in ambient air also produce this on the reaction with  $\text{NO}^+$  and  $\text{O}_2^+$ . Issues using this method have however been reported by Syft as most hydrocarbons produce the  $m/z$  43 ion (also produced by  $\text{O}_2^+$  impurity reagent ions in the flow tube in the  $\text{NO}^+$  mode), which inevitably interfere with the accurate initial quantification of acetaldehyde.

**3.7.2 Quantification using  $\text{OH}^-$  only.** Based on the kinetic data obtained in the present study, it is possible to propose a method of quantification for ethylene oxide in the presence of acetaldehyde using the  $\text{OH}^-$  reagent ion and the  $m/z$  59 product ion for ethylene oxide, and  $m/z$  43 for acetaldehyde. This is relatively straightforward as there are no direct product ion overlaps. Thus, the values from Tables 1 and 2 were entered into the Syft Voice200*infinity* instrument library and a validation experiment was performed to test for possible cross sensitivity issues. In this experiment, ethylene oxide and acetaldehyde were added separately to a Nalophan bag filled with dry zero-air whilst the concentrations of both compounds were analysed using the new library entries. As can be seen from Fig. 3A, the measured ethylene oxide concentration remains below 50 ppbv when acetaldehyde is added up to 500 ppbv. This is due to an increase in ion signal at  $m/z$  59 corresponding to less than 0.5% of acetaldehyde product ions possibly due to an impurity. In a complementary test when ethylene oxide is added up to 2000 ppbv, no noticeable increase of calculated acetaldehyde concentration is observed (Fig. 3B).

It is important to consider that  $\text{CO}_2$  is present in breath and ambient air and will undoubtedly be present in the samples

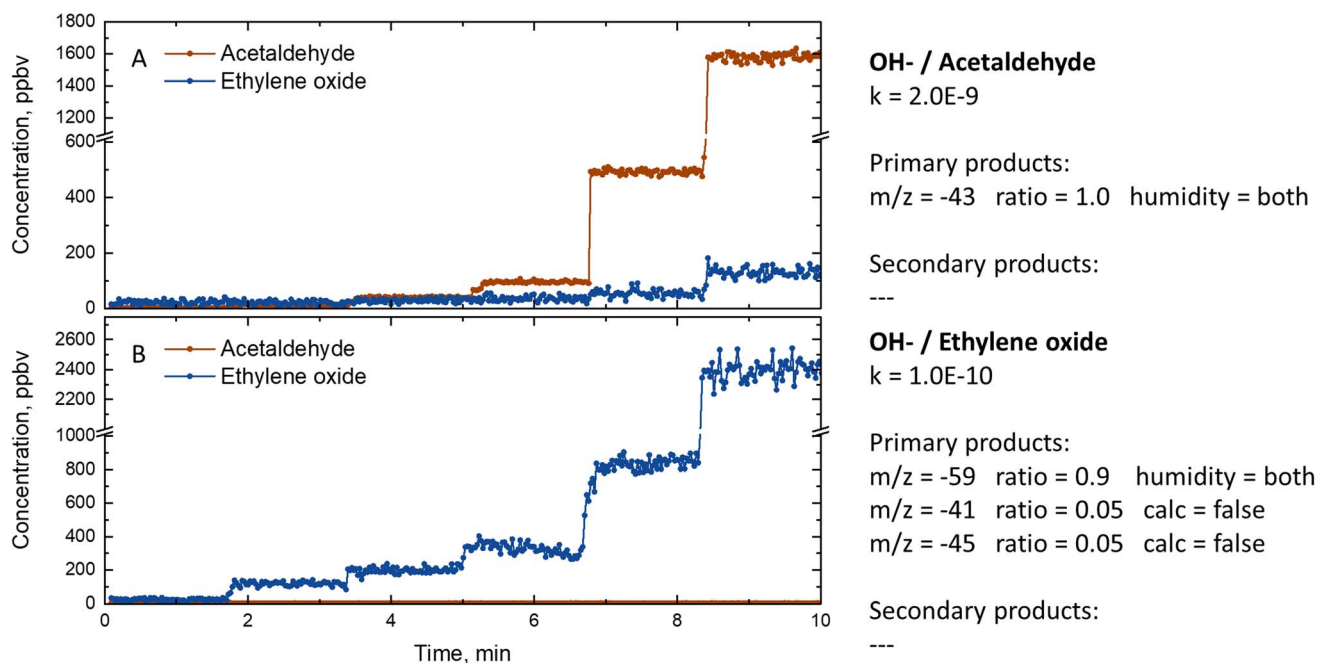


Fig. 3 Quantification of ethylene oxide and acetaldehyde using the  $\text{OH}^-$  reagent ion only. (A) The calculated concentrations when acetaldehyde is introduced in stepwise increased concentration. (B) Concentrations calculated when ethylene oxide is introduced in the absence of acetaldehyde.



**Table 2** The rate coefficients for the ion–molecule reactions of interest for the SIFT-MS analyses of acetaldehyde and ethylene oxide. Also given are the dipole moments and polarisability values<sup>39</sup> used to calculate  $k_c$

| Compound  | MW | $D$ Debye | $\alpha$ $10^{-24}$ cm <sup>3</sup> | H <sub>3</sub> O <sup>+</sup> [ $k_c$ ] <sup>a</sup> | NO <sup>+</sup> $k$ , [ $k_c$ ] <sup>a</sup> | OH <sup>−</sup> $k$ , [ $k_c$ ] <sup>a</sup> | O <sup>−</sup> $k$ , [ $k_c$ ] <sup>a</sup> |
|---|----|-----------|-------------------------------------|--|--|--|---|
| Acetaldehyde<br>CH <sub>3</sub> CHO               | 44 | 2.69      | 4.59                                | [3.4]  | 0.6 [2.9]                                    | 2.0 [3.5]                                    | 0.2 [3.6]                                   |
| Ethylene oxide<br>C <sub>2</sub> H <sub>4</sub> O | 44 | 1.89      | 4.43                                | [2.6]  | 0.1 [2.2]                                    | 0.1 [2.7]                                    | 1.7 [2.8]                                   |

<sup>a</sup>  $k$  and  $k_c$  are given in the units of  $10^{-9}$  cm<sup>3</sup> s<sup>−1</sup>, with  $k_c$  in square brackets.

**Table 3** The LOD and LOQ values for the reactions of acetaldehyde and ethylene oxide with the OH<sup>−</sup> reagent ions when using the Voice200*infinity* instrument obtained for the average across 180 data points recorded, with total method dwell time indicated

| Compound       | Time limit (ms) | LOD (ppbv) | LOQ (ppbv) |
|----------------|-----------------|------------|------------|
| Acetaldehyde   | 100             | 1.1        | 3.2        |
|                | 500             | 0.5        | 1.4        |
|                | 1000            | 0.3        | 1.0        |
| Ethylene oxide | 100             | 12.8       | 38.6       |
|                | 500             | 6.0        | 18.2       |
|                | 1000            | 4.0        | 12.1       |

being analysed by SIFT-MS users (unless they work under an inert atmosphere – a very uncommon use case). Tests were thus completed to investigate whether CO<sub>2</sub> would react with the OH<sup>−</sup> reagent ion to produce any false positive results or extra products. Our results indicated that no significant extra peaks are present when ethylene oxide and CO<sub>2</sub> are together in the presence of OH<sup>−</sup> (when compared to zero-air), at breath relevant CO<sub>2</sub> concentrations (*ca.* 6%). In zero-air, a signal was observed at  $m/z$  61, although according to the previous literature this was most likely due to the first hydrate of OH<sup>−</sup> (OH<sup>−</sup>H<sub>2</sub>O), producing the HCO<sub>3</sub><sup>−</sup> artefact.<sup>44,45</sup> This does not however interfere with ethylene oxide.

Therefore, in summary, OH<sup>−</sup> is a potential reagent ion to use for the accurate measurement of ethylene oxide in the presence of high acetaldehyde, due to (i) the lack of any overlapping peaks from different branching pathways of the ethylene oxide and acetaldehyde reactions, and (ii) the significant differences in rate coefficients between these two reactions. Note, however, that the use of the product ion  $m/z$  59 is potentially subject to overlap with the product ions from propanol isomers or other compounds. Hence this method needs to be tested for each matrix and propanol would potentially need to be monitored by other reagent ions (followed by subtraction).

### 3.8 Limit of detection and quantification analysis

The LOD is required to be low enough for ethylene oxide and acetaldehyde to be detected within sesame seed derived products as well as in ambient air. It is also required to be lower than the recommended exposure limit of 1 ppm (8 hour time weighted average) of ethylene oxide, as given by the Occupational Safety and Health Administration (OSHA). The LOD and

LOQ values were calculated by incorporating the observed rate constants and branching ratios from Tables 1 and 2 into the Syft Voice200*infinity* library for calculation of concentrations of ethylene oxide and acetaldehyde.

The LOD for ethylene oxide and acetaldehyde were determined from repeated blank background analyses. The SIM mode on the Voice200*infinity* was utilised in which 180 data points were recorded by the instrument using a blank glass vessel with zero-air flowing through it. These measurements were repeated for the reagent ions of interest (OH<sup>−</sup> and O<sup>−</sup>) for ethylene oxide and acetaldehyde detection. The standard deviation was taken for each measurement and the LOD was calculated by multiplying this standard deviation by 3.3 for the LOD and by 10 for the LOQ. The results for the LOD and LOQ are shown in Table 3.

## 4 Conclusion

SIFT-MS has the potential to accurately quantify ethylene oxide in the presence of acetaldehyde using three alternative approaches. Firstly, by combining H<sub>3</sub>O<sup>+</sup> (product ions at  $m/z$  45) and NO<sup>+</sup> (product ions at  $m/z$  43) analyses; secondly, by using a product ion from OH<sup>−</sup> at  $m/z$  59; and lastly by O<sup>−</sup>, by combining  $m/z$  41 and 43 product ions. It must, however, be emphasised that a blank correction should also always be conducted. We found that the most accurate SIFT-MS analyses can be achieved using the OH<sup>−</sup> reagent ion, as this leads to nonoverlapping product ions. SIFT-MS may thus be applied to the high throughput rapid analyses of food samples to ensure their safety concerning possible ethylene oxide contamination. The other methods using H<sub>3</sub>O<sup>+</sup> and NO<sup>+</sup>, as well as O<sup>−</sup> are prone to greater uncertainty. The results of this study suggest that other isobaric species may be quantified using SIFT-MS (with negative ions and a nitrogen carrier gas), such as traces of formic acid in the presence of large concentrations of ethanol.

## Conflicts of interest

Ann-Sophie Lehnert, Nicholas Demarais, Vaughan S. Langford and Leslie P. Silva are employees at Syft Technologies entities in Germany, New Zealand and the United States of America. Mark J. Perkins is an employee at Element Lab Solutions (formerly Anatune) in the United Kingdom. Syft Technologies is a manufacturer of SIFT-MS instruments (including the Voice200 series



described in this article) and Element Lab Solutions is a distributor of SIFT-MS instruments in both the United Kingdom and the Republic of Ireland.

## Acknowledgements

The authors gratefully acknowledge financial support from the Czech Science Foundation (Grantová Agentura České Republiky, GACR; Project No. 21-25486S) and from the *Praemium Academiae* funding by the Czech Academy of Sciences.

## References

- 1 P. P. McClellan, Manufacture and uses of ethylene oxide and ethylene glycol, *Ind. Eng. Chem.*, 1950, **42**, 2402–2407.
- 2 A. Dudkiewicz, P. Dutta and D. Kolożyn-Krajewska, Ethylene oxide in foods: current approach to the risk assessment and practical considerations based on the European food business operator perspective, *Eur. Food Res. Technol.*, 2022, **248**, 1951–1958.
- 3 A. C. Leslie Silva, Chad Bastian, Christopher Williams, Zachary Morseth, and Elliott Franco, *Simple, Rapid Analysis of Ethylene Oxide in a Polysorbate 80 Excipient Using SIFT-MS*, 2023, <https://bit.ly/3QLWRmC>.
- 4 O. Frost, *Quantitative Ethylene Oxide Analysis in Polysorbate 80*, 2023, <https://www.azom.com/article.aspx?ArticleID=22192>.
- 5 G. C. C. Mendes, T. R. S. Brandão and C. L. M. Silva, Ethylene oxide sterilization of medical devices: a review, *Am. J. Infect. Control*, 2007, **35**, 574–581.
- 6 G. C. Mendes, T. R. S. Brandão and C. L. M. Silva, in *Sterilisation of Biomaterials and Medical Devices*, ed. S. Lerouge and A. Simmons, Woodhead Publishing, 2012, DOI: [10.1533/9780857096265.71](https://doi.org/10.1533/9780857096265.71), pp. 71–96.
- 7 F. Wesley, B. Rourke and O. Darbishire, The formation of persistent toxic chlorohydrins in foodstuffs by fumigation with ethylene oxide and with propylene oxide, *J. Food Sci.*, 1965, **30**, 1037–1042.
- 8 M. W. Ballard and N. S. Baer, Ethylene oxide fumigation: results and risk, *Assessment*, 1986, **7**, 143–168.
- 9 F. Tateo and M. Bononi, Determination of ethylene chlorohydrin as marker of spices fumigation with ethylene oxide, *J. Food Compos. Anal.*, 2006, **19**, 83–87.
- 10 R. B. Harvey, Use of ethylene oxide for the eradication of pests, *Science*, 1931, **73**, 100–101.
- 11 OSHA, *Regulatory Review of the Occupational Safety and Health Administration's Ethylene Oxide Standard*, Office of Evaluations and Audit Analysis, 200 Constitution Ave., N.W. Washington, D.C. 20210, 2005.
- 12 T. Bessaire, T. Stroheker, B. Eriksen, C. Mujahid, Y.-A. Hammel, J. Varela, T. Delatour, A. Panchaud, P. Mottier and R. H. Stadler, Analysis of ethylene oxide in ice creams manufactured with contaminated carob bean gum (E410), *Food Additi. Contam.: Part A*, 2021, **38**, 2116–2127.
- 13 S. Rebsdats and D. Mayer, *Ethylene Oxide*, Ullmann's Encyclopedia of Industrial Chemistry, 2000.
- 14 E. M. Tompkins, K. I. E. McLuckie, D. J. L. Jones, P. B. Farmer and K. Brown, Mutagenicity of DNA adducts derived from ethylene oxide exposure in the pSP189 shuttle vector replicated in human Ad293 cells, *Mutat. Res., Genet. Toxicol. Environ. Mutagen.*, 2009, **678**, 129–137.
- 15 V. L. Dellarco, W. M. Generoso, G. A. Sega, J. R. Fowle III, D. Jacobson-Kram and H. E. Brockman, Review of the mutagenicity of ethylene oxide, *Environ. Mol. Mutagen.*, 1990, **16**, 85–103.
- 16 M. J. M. Nivard, K. Czene, D. Segerbäck and E. W. Vogel, Mutagenic activity of ethylene oxide and propylene oxide under XPG proficient and deficient conditions in relation to N-7-(2-hydroxyalkyl)guanine levels in *Drosophila*, *Mutat. Res., Fundam. Mol. Mech. Mutagen.*, 2003, **529**, 95–107.
- 17 C. R. Kirman, A. A. Li, P. J. Sheehan, J. S. Bus, R. C. Lewis and S. M. Hays, Ethylene oxide review: characterization of total exposure via endogenous and exogenous pathways and their implications to risk assessment and risk management, *J. Toxicol. Environ. Health, Part B*, 2021, **24**, 1–29.
- 18 E. Salinas, L. Sasich, D. H. Hall, R. M. Kennedy and H. Morriss, Acute ethylene oxide intoxication, *Drug Intell. Clin. Pharm.*, 1981, **15**, 384–386.
- 19 B. B. Gollapudi, S. Su, A. A. Li, G. E. Johnson, R. Reiss and R. J. Albertini, Genotoxicity as a toxicologically relevant endpoint to inform risk assessment: a case study with ethylene oxide, *Environ. Mol. Mutagen.*, 2020, **61**, 852–871.
- 20 A. Kolman, M. Chovanec and S. Osterman-Golkar, Genotoxic effects of ethylene oxide, propylene oxide and epichlorohydrin in humans: update review (1990–2001), *Mutat. Res., Rev. Mutat. Res.*, 2002, **512**, 173–194.
- 21 F. Li, A. Segal and J. J. Solomon, *In vitro* reaction of ethylene oxide with DNA and characterization of DNA adducts, *Chem.-Biol. Interact.*, 1992, **83**, 35–54.
- 22 J. J. Solomon, *Cyclic Adducts and Intermediates Induced by Simple Epoxides*, IARC Sci. Publ., 1999, pp. 123–135.
- 23 A. Kolman, M. Näslund and C. J. Calleman, Genotoxic effects of ethylene oxide and their relevance to human cancer, *Carcinogenesis*, 1986, **7**, 1245–1250.
- 24 J. A. Swenberg, A. Ham, H. Koc, E. Morinello, A. Ranasinghe, N. Tretyakova, P. B. Upton and K.-Y. Wu, DNA adducts: effects of low exposure to ethylene oxide, vinyl chloride and butadiene, *Mutat. Res., Genet. Toxicol. Environ. Mutagen.*, 2000, **464**, 77–86.
- 25 J.-C. Juncker, *Commission Regulation (EU) 2015/868 of 26 May 2015 Amending Annexes II, III and V to Regulation (EC) No 396/2005 of the European Parliament and of the Council as Regards Maximum Residue Levels for 2,4,5-T, Barban, Binapacryl, Bromophos-Ethyl, Campechlor (Toxaphene), Chlorbufam, Chloroxuron, Chlozolinate, DNOC, Di-allate, Dinoseb, Dinoterb, Dioxathion, Ethylene Oxide, Fentin Acetate, Fentin Hydroxide, Flucycloxuron, Flucythrinate, Formothion, Mecarbam, Methacrifos, Monolinuron, Phenothrin, Propham, Pyrazophos, Quinalphos, Resmethrin, Tecnazene and Vinclozolin in or on Certain Products*, Official Journal of the European Union, 2015, p. 145.



- 26 A. Kowalska and L. Manning, Food safety governance and guardianship: the role of the private sector in addressing the EU ethylene oxide incident, *Foods*, 2022, **11**, 204.
- 27 T. Cucu, F. David and C. Devos, Analysis of ethylene oxide and 2-chloroethanol in food products: challenges and solutions, *Column*, 2022, **18**, 10–16.
- 28 D. Smith, P. Španěl, N. Demarais, V. S. Langford and M. J. McEwan, Recent developments and applications of selected ion flow tube mass spectrometry, SIFT-MS, *Mass Spectrom. Rev.*, 2023, e21835, DOI: [10.1002/mas.21835](https://doi.org/10.1002/mas.21835).
- 29 T. Miyake and T. Shibamoto, Quantitative analysis of acetaldehyde in foods and beverages, *J. Agric. Food Chem.*, 1993, **41**, 1968–1970.
- 30 B. Altemose, J. Gong, T. Zhu, M. Hu, L. Zhang, H. Cheng, L. Zhang, J. Tong, H. M. Kipen, P. O. Strickland, Q. Meng, M. G. Robson and J. Zhang, Aldehydes in relation to air pollution sources: a case study around the Beijing Olympics, *Atmos. Environ.*, 2015, **109**, 61–69.
- 31 D. M. Jackson, N. G. Adams and L. M. Babcock, Ion-molecule reactions of several ions with ethylene oxide and propenal in a selected ion flow tube, *J. Am. Soc. Mass Spectrom.*, 2007, **18**, 445–452.
- 32 D. Smith, M. J. McEwan and P. Španěl, Understanding gas phase ion chemistry is the key to reliable selected ion flow tube-mass spectrometry analyses, *Anal. Chem.*, 2020, **92**, 12750–12762.
- 33 P. Španěl, Y. F. Ji and D. Smith, SIFT studies of the reactions of  $\text{H}_3\text{O}^+$ ,  $\text{NO}^+$  and  $\text{O}_2^+$  with a series of aldehydes and ketones, *Int. J. Mass Spectrom.*, 1997, **165**, 25–37.
- 34 D. Hera, V. S. Langford, M. J. McEwan, T. I. McKellar and D. B. Milligan, Negative reagent ions for real time detection using SIFT-MS, *Environments*, 2017, **4**, 16.
- 35 D. Smith and N. G. Adams, The selected ion flow tube (SIFT): studies of ion-neutral reactions, *Adv. Atomic Mol. Phys.*, 1988, **24**, 1–49.
- 36 K. Sovová, K. Dryahina and P. Španěl, Selected ion flow tube (SIFT) studies of the reactions of  $\text{H}_3\text{O}^+$ ,  $\text{NO}^+$  and  $\text{O}_2^+$  with six volatile phytochemical esters, *Int. J. Mass Spectrom.*, 2011, **300**, 31–38.
- 37 T. Su and W. J. Chesnavich, Parametrization of the ion–polar molecule collision rate constant by trajectory calculations, *J. Chem. Phys.*, 1982, **76**, 5183–5185.
- 38 G. Bouchoux, J. Y. Salpin and D. Leblanc, A relationship between the kinetics and thermochemistry of proton transfer reactions in the gas phase, *Int. J. Mass Spectrom. Ion Processes*, 1996, **153**, 37–48.
- 39 *CRC Handbook of Chemistry and Physics*, ed. R. C. Weast, M. J. Astle and W. H. Beyer, CRC Press, Boca Raton, 66<sup>th</sup> edn, 1985.
- 40 F. Neese, Software update: the ORCA program system—Version 5.0, *Wiley Interdiscip. Rev. Comput. Mol. Sci.*, 2022, **12**, e1606.
- 41 M. D. Hanwell, D. E. Curtis, D. C. Lonie, T. Vandermeersch, E. Zurek and G. R. Hutchison, Avogadro: an advanced semantic chemical editor, visualization, and analysis platform, *J. Cheminform.*, 2012, **4**, 17.
- 42 E. Caldeweyher, C. Bannwarth and S. Grimme, Extension of the D3 dispersion coefficient model, *J. Chem. Phys.*, 2017, **147**, 034112.
- 43 E. P. L. Hunter and S. G. Lias, Evaluated gas phase basicities and proton affinities of molecules: an update, *J. Phys. Chem. Ref. Data*, 1998, **27**, 413–656.
- 44 M. Ghislain, N. Costarramone, T. Pigot, M. Reyrolle, S. Lacombe and M. Le Bechec, High frequency air monitoring by selected ion flow tube-mass spectrometry (SIFT-MS): influence of the matrix for simultaneous analysis of VOCs,  $\text{CO}_2$ , ozone and water, *Microchem. J.*, 2020, **153**, 104435.
- 45 A. B. Raksit and D. K. Bohme, An experimental-study of the influence of hydration on the reactivity of the hydroxide anion in the gas-phase at room-temperature, *Can. J. Chem.*, 1983, **61**, 1683–1689.

